Proceedings World Geothermal Congress 2020+1
Reykjavik, Iceland, April - October 2021

The 3D Seismic Velocity Model and Hypocenter Relocation Results of Patuha Geothermal Field

Akhmad Fanani Akbar, Reza Jamil Fajri, Chevy Iskandar, Randy Wijaya Atmaja

akhmad@geodipa.co.id

Keywords: Patuha, micro sesimic, hypocenter, velocity, tomography

ABSTRACT

Geothermal reservoir monitoring using micro seismic survey has been implemented recently in several geothermal fields in Indonesia. Micro seismic survey has been conducted from January 1st until later April 1st 2018 in Patuha Geothermal Field using 9 seismometers that are placed near well locations and fault distribution. 654 micro seismic events (ts-tp less than 3 second) and 640 regional (ts-tp more than 5 second) was identified in this period, but only 491 micro seismic events have clear onset of P and S waves arrival time. Initial location is determined using NonLinLoc algorithm and will be used as input for Velest program to obtain 1D velocity model. Double difference seismic tomography is applied to jointly determine relocation hypocenter and 3D seismic velocity model (Vp, Vs, & Vp/Vs). The aim 3D seismic velocity model determination is to infer reservoir condition, because Vp/Vs ratio is sensitive with sub-surface variations in rock and fluid properties. The results show hypocenter location (depth 0-500 masl) is correlated with existing production zone with high permeability and main fault direction. It is expected to support well targeting for the next development stage of Patuha geothermal field.

1. GEOLOGY PATUHA

The Patuha field is situated within a northwest-trending volcanic mountain range, including the nearby peaks of North Patuha (2414 m); South Patuha (2390 m); Urug (2201 m) and Walang (2178m) (Layman et.al., 2003). The structure in Patuha Field is dominated by NE-SW (Alamendah Fault, Cibuni Crater Fault, Ciwidey Crater Fault, Tiis Fault, and Dewata Fault) and NW-SE (Rancabali Fault, Patenggang Fault, Ciwidey Crater Fault, Urug Fault, Tiis Fault, and Dewata Fault) in line with Meratus and Sumatera trend (Figure 1). The type of lithology in Patuha geothermal field consist of lavas, tuff, and breccia. Diorite or micro-diorite intrusive cut the volcanic section in some wells. Surface manifestations in Patuha consist of fumaroles, thermal springs, and cold gas discharges. These include the three fumarole areas at Kawahs Cibuni, Putih and Ciwidey. Thermal springs have been identified at lower elevations on the south, west and northwest flank of the volcanic highland. An area of cold gas discharge is present between Kawah Ciwidey and Kawah Putih, and also on the south flank of the volcanic highland.

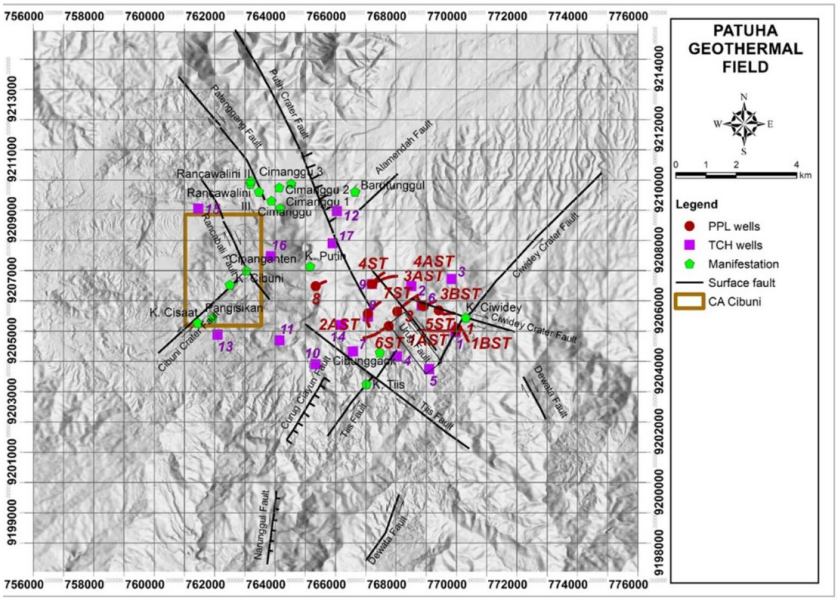

Figure 1: Fault distribution, production & injection well, and manifestation in Patuha Geothermal Field (Elfina, 2017)

2. DATA & INSTRUMENTATION

We have deployed 6 (six) MEQ station as agreed in Terms of Reference (Term of Reference). The 3 (three) spare station were also deployed as additional stations, so that 9 (nine) station were successfully deployed on 4 January 2018. On 4 February 2018, 2 (two) additional instruments (surface type) were also installed in the designated place as a additional station. Therefore, a total of 11 (eleven) stations was deployed in the survey area.

Several parameters were set to fulfill the survey specification in terms of reference: sampling frequency was set to 200Hz, the high gain mode was used, and the raw data were set to have 1 hour of record length. The parameter of the recording could be seen in Table.

The 2 (two) additional additional stations are the surface type, so the sensors were placed on the surface with different specification. Those additional stations used similar recording parameter. Prior of installation, we have calibrated all of the instruments to ensure the data will be processed in correct manner. Data and instruments calibration took place in PPL-7 wellpad. We also did calibration for 2 (two) additional stations separately in Bandung basecamp prior of its deployment.

3. DATA PROCESSING

3.1 Seismic Event Identification

Seismic data recording has been conducted for 94 days continuously from January 1 to April 4, 20018 using 11 Seismometer stations. A total number of 654 micro-earthquake (MEQ) were identified. That event is recorded by a minimum of 3 stations. The average is 7 events/day were identified. From 654 events, only 491 events could be picked. The others were not clear (noisy), so it can't be picked. The processing was carried out using SeisGram2k7 by Anthony Lomax (Lomax, et al., 2000) for detection of seismic events and phase picking (P and S arrival time). Event detection and picking arrival time of P and S-wave phase were done visually (using the eyes, hour to hour, minute to minute). Quality control of picked arrival time was done by assessing Vp/Vs ratio (Vp/Vs ratio = 1.73) from Wadati Diagram for each event. All the picked events, the arrival time of P and S-wave made into a list of event catalogs.

The signal identification is carried out visually using software *Seisgram2K v.60*. Regional-earthquake signal has a difference of S and P phase about 17 seconds (Figure 2) and micro-earthquake signal about less than 3 seconds (Figure 3), the identified signal at least recorded by 3 stations for an accurate hypocenter location.

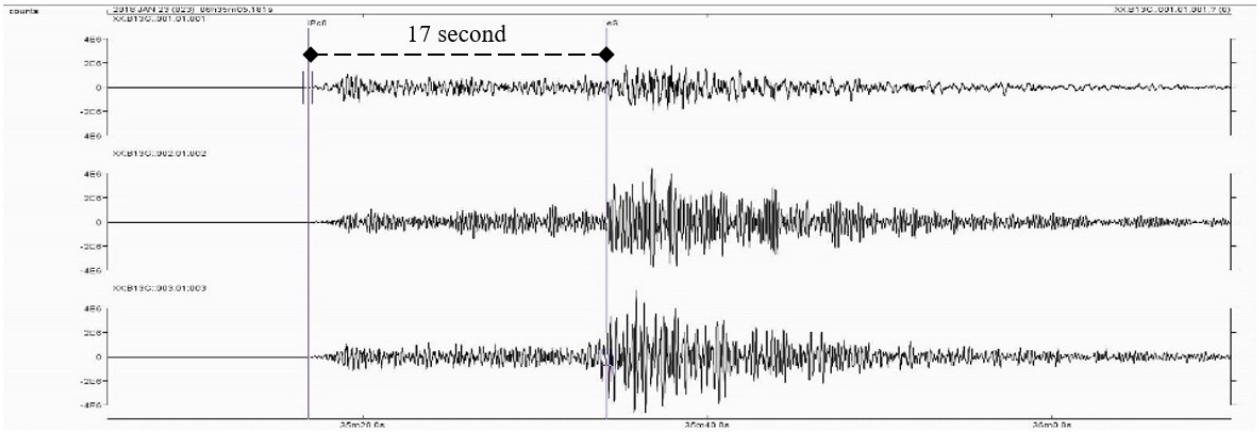

Figure 2: Example of Regional event occurred on January 23, 2018, at 06:35:16 UTC time (+7 hours for local time) at station B13C. Red arrow show Ts-Tp = 17 s.

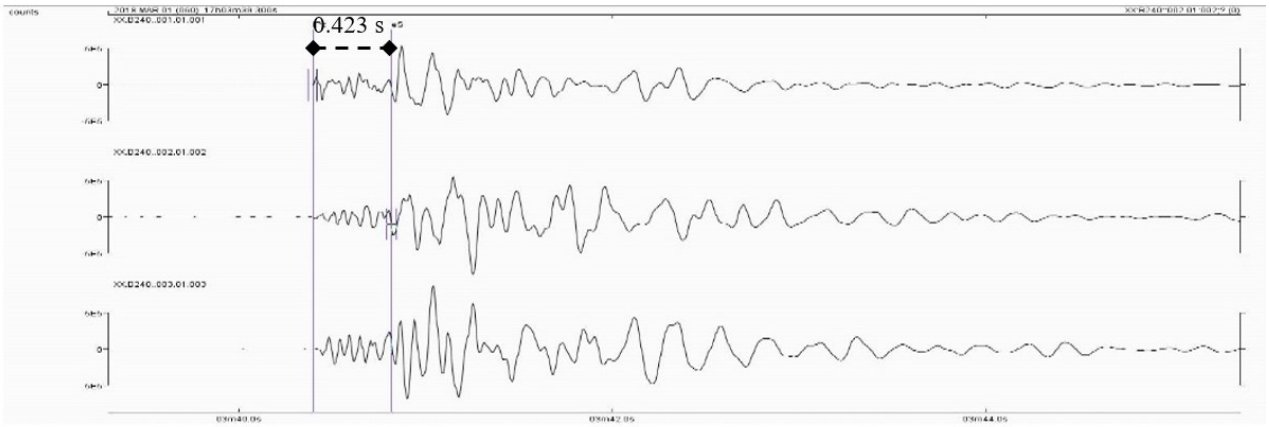

Figure 3: Example of MEQ event occurred on March 1, 2018, at 17:03:40 UTC time (+7 hours for local time) at station B240. Red arrow shows Ts-Tp = 0.423s. The seismograms show the three components (one vertical and two horizontal).

3.2 Hypocenter Determination

From data recording for 94 days (January 1-April 4) in Patuha geothermal field, totally we have been successfully identified and picked of arrival times P and S-waves phases of 491 MEQ events. These numbers of events are equivalent to 3,048 P-wave phases, 2,815 S-wave phases and 2,694 pairs of P and S-wave phases from eleven seismometers. Most of MEQ events have difference of arrival P and S (ts-tp) less than three seconds. Wadati diagram curve, plot of P-wave travel times versus S-wave travel times, shows that vp/vs ratio is around 1.69. All of these data such as arrival times, stations coordinate as well as 1D velocity model will be used as input in NonLinLoc software to determine initial hypocenter locations.

The initial 1D velocity model that used in this study base on the result of previous research 3D velocity structures in Wayang Windu Geothermal field (Palgunadi, 2017). Palgunadi's research used MEQ data that was recorded through 2015 from 45 seismometers. We

use Palgunadi research results because we lack geological information around Patuha geothermal field. We assume that Wayang Windu have geological similarity features with Patuha.

3.3 1D Velocity Determination

The 1D velocity model determination was performed using VELEST computer program (Kissling et, al., 1995) to update the initial 1D velocity model. The input data of VELEST software are initial velocity models (*Vp* and *Vs*), hypocenter models from previous NonLinLoc hypocenter determination result (hypocenter coordinate, depth, and origin time), and station locations.

We used the result of 3D velocity structures research of Wayang Windu Geothermal field (Palgunadi, 2017) to obtain the initial 1D velocity model. The initial velocity model was processed using MATLAB computer program to randomly generate 100 starting velocity models as VELEST input. Then, each model was processed using VELEST software by applying ten different velocity damping parameters (0.01 to 1.0). The VELEST output with smallest RMS was selected as the best final velocity model.

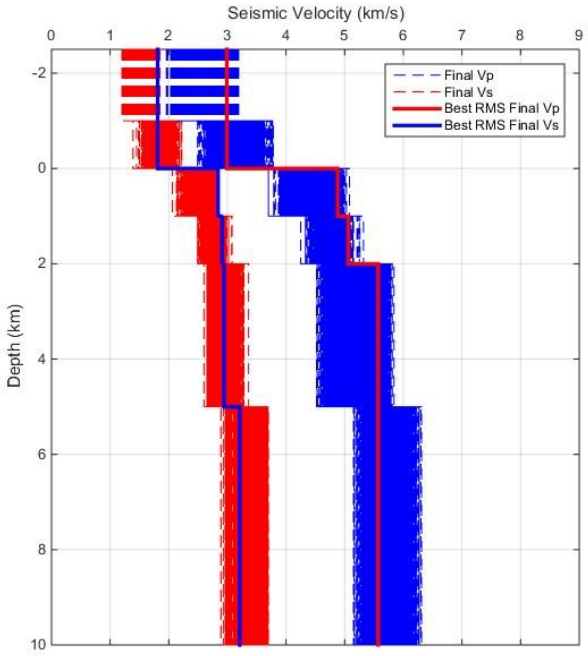

Figure 4: The VELEST outputs of 1000 initial velocity models. Updated 1D seismic velocity model compared to its initial model.

3.4 Hypocenter and Velocity Model Joint Inversion

Double difference seismic tomography is applied to jointly determine relocation hypocenter and 3D seismic velocity model (Vp, Vs, & Vp/Vs). The aim 3D seismic velocity model determination is to infer reservoir condition, because Vp/Vs ratio is sensitive with sub-surface variations in rock and fluid properties. We used initial hypocenter location from previous calculation and 1D velocity model that is determined before with VELEST.

4. RESULTS & DISCUSSION

The results of hypocenter determination using NonLinLoc (Lomax, 2000) and TomoDD (Zhang and Thurber, 2003), in lateral distribution is not too different, but in vertical distribution the hypocenter distribution from TomoDD is deeper than NonLinLoc. The hypocenter location of micro seismic events is located beneath around well trajectory (injection and production well) and fault. Two compartment of micro seismic events (Area I and Area II) and its boundaries are interpreted with Urug Fault as separator of those compartments. Northern boundary of Area II is Ciwidey II Fault (NE-SW) and southern boundary of Area II is Ciwidey Creater Fault (NW-SE) that is identified from remote sensing analysis in previous study (Pradipta, 2016). Micro seismic events in Area I is around trajectory of three production wells and in Area II is around injection well and production.

3D seismic velocity model determination is to infer reservoir condition, because Vp/Vs ratio is sensitive with sub-surface variations in rock and fluid properties. To determine area that is has high resolution we used Derivative weighted sum (DWS). Because it is representation of total weighted ray length in cell and ray density pass close to grid note. The high anomaly of DWS for P Wave and S Wave Velovity is distributed in area II, the area with high distribution of MEQ events and also around production well. In area with high anomaly of DWS, we interpreted that high Vp/Vs values is representation of steam content. Because in area II, the steam content of production well is higher than in Area II.

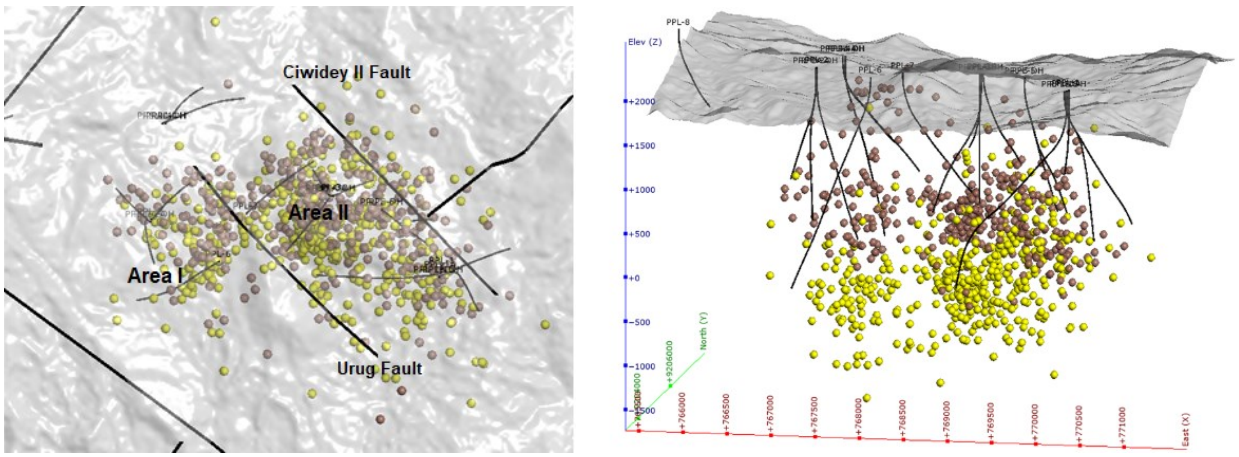

Figure 5: Hypocenter Distribution based on NonLinLoc calculation (grey) and TomoDD results (yellow) overlaid with geological structure

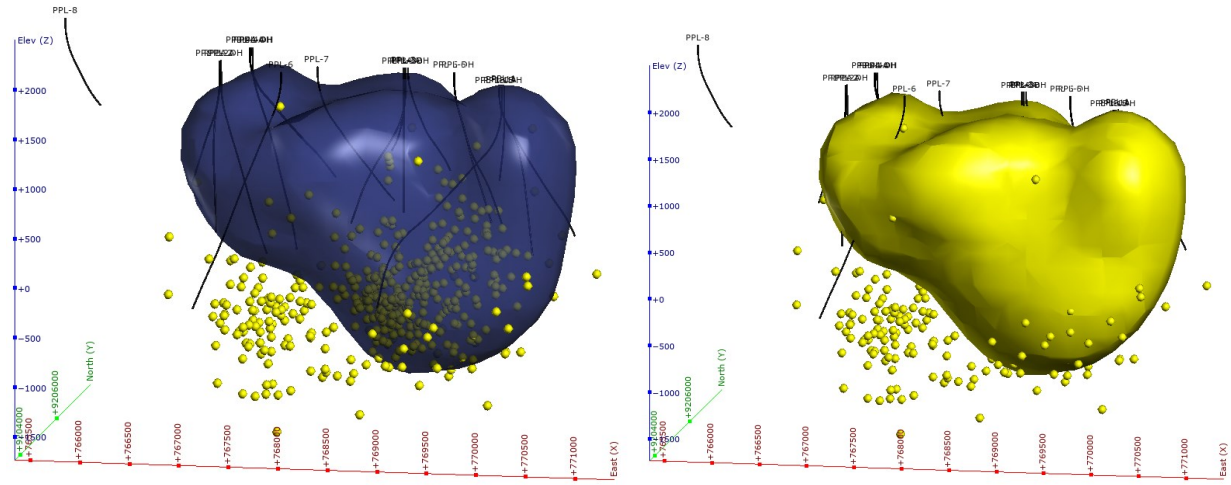

Figure 5: High isosurface derivative weight sum (DWS) for P Wave (left) and S Wave Velocity (right)

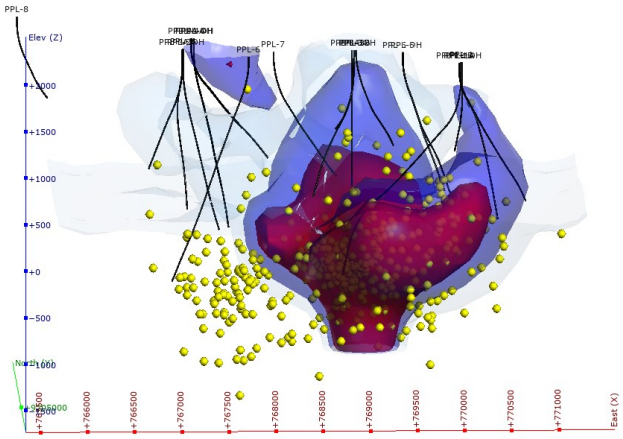

Figure 6: Distribution of Vp/Vs values isosurface, Vp/Vs 1.57 (red), Vp/Vs 1,62 (dark blue), Vp/Vs 1,67 (light blue)

REFERENCES

Elfina, (2017). Updated Conceptual Model of The Patuha Geothermal Field, Indonesia. UNU-GTP, Iceland, report 2017, number 10.

Lomax, A., J. Virieux, P. Volant, and C. Thierry-Berge (2000). Probabilistic earthquake location in 3D and layered models, in Advances in Seismic Event Location, C. H. Thurber and N. Rabinowitz (Editors), Kluwer Academic Publishers, Dordrecht/Boston/London, 101–134.Kissling, E., Ellsworth W.L., Eberhart-Phillips D., and Kradolfer U. (1994), J. Geophys. Res, 99, 19635-19646.

Kissling, E., (1995), Program VELEST USER'S GUIDE – Short Introduction, Zurich: ETH Zuerich, 1-31.

Layman, E.B., and Soemarinda, S., 2003: The Patuha vapor-dominated resource West Java, Indonesia. Proceeding of the 28th Workshop on Geothermal Reservoir Engineering, Stanford University, Stanford, Ca, 10 pp.

Lomax, A., and A. Curtis (2001), "Fast, probabilistic earthquake location in 3D models using Oct-Tree Importance sampling". Geophys. Res. Abstr., 3.

Palgunadi, K.H., Nugraha, A.D., Sule, M.R., and Meidiana T. (2017). Steam and Brine Zone Prediction around Geothermal Reservoir Derived from Delay Time Seismic Tomography and Anisotropy Case Study: "PR" Geothermal Field. Southeast Asian Conference on Geophysics

Pradipta, R. A., (2016), Penentuan Zona Permeabilitas Menggunakan Citra ALOS Palsar, Pemetaan Geologi, dan Geokimia Tanah dan Udara Tanah (Hg-CO2), Studi Kasus Lapangan Panasbumi Ciwidey, Kabupaten Bandung, Tesis Magister, Institut Teknologi Bandung

Zhang, H., dan C. H. Thurber., 2003. User's manual for tomoDD1.1 (double difference tomography) for determining event locations and velocity structure from local earthquake and explosions,draft, University of Wisconsin-Madison.

Zhang, H., dan C. H. Thurber, 2003. Double difference tomography: The method and its application to the Hayward Fault, California: Bull. Seism. Soc. Am., 93,1875-1889.